Day-Ahead Dispatch of Integrated Electricity and Natural Gas System Considering Reserve Scheduling and Renewable Uncertainties

Fan Liu [ID], *Student Member, IEEE*, Zhaohong Bie [ID], *Senior Member, IEEE*, and Xu Wang, *Student Member, IEEE*

Abstract—For secure operation of integrated electricity and natural gas system (IEGS), reserve is a useful support to manage renewable uncertainties and $N-1$ contingencies. Thus, a day-ahead economic dispatch model of IEGS with reserve scheduling is presented in this paper. Considering the uncertainty of gas flow direction, a novel second-order cone (SOC) relaxation of Weymouth equation is designed to address the nonconvexity. Then, the proposed robust nonconvex model is mathematically transformed into a solvable mixed integer second-order cone programming (MISOCP) problem. To guarantee the tightness of SOC relaxation and achieve accurate dispatch solutions, MISOCP results are corrected accordingly by the multi-slack-node gas flow calculation with the Newton–Raphson method. Numerical cases are performed on IEEE 39-bus-15-node and IEEE 118-bus-40-node test IEGSs, demonstrating the proposed approach is feasible and effective for exact IEGS day-ahead dispatch and the proposed MISOCP model can provide a more economic dispatch solution with a shorter computational time than conventional MISOCP and mixed integer linear programming (MILP) models.

Index Terms—Day-ahead economic dispatch, integrated electricity and natural gas system (IEGS), reserve scheduling, renewable uncertainty, second-order cone (SOC) relaxation.

NOMENCLATURE

Sets and Indices

i, N_g	Index, number of gas-fired generators (GGs) with self-owned natural gas tanks (SNGTs)
j, N_c	Index, number of coal-fired generators (CGs)
s, N_r	Index, number of renewable resources
b, N_b	Index, number of electricity network buses
t, N_t	Index, number of dispatch periods
k	Index of electricity transmission lines
u, N_{sp}	Index, number of gas suppliers
q, N_{com}	Index, number of compressors
p, N_f	Index, number of pipelines

n, l, l'	Indices of natural gas network nodes
m	Index of $N-1$ generator outages

Variables

$P_{i,t}^g, A_{i,t}^g, R_{i,t}^g$	Scheduled power, regulation reserve (RR) and spinning reserve (SR) of GG i for period t
$P_{j,t}^c, A_{j,t}^c, R_{j,t}^c$	Scheduled power, RR and SR of CG j for period t
$Pl_{k,t}^0, Pl_{k,t}$	Power flow without and with uncertainties of transmission line k for period t
$E_{b,t}$	Total forecast error of renewable power and electricity load at bus b for period t
$L_{n,t}^g$	Gas load at node n for period t
$S_{u,t}$	Natural gas output of gas supplier u for period t
$G_{i,t}^g, G_{i,t}^a, G_{i,t}^r$	GG i's gas demand of power, RR, SR for period t
$Fl_{p,t}$	Natural gas flow of pipeline p for period t
$F_{q,t}^{com}$	Natural gas flow of compressor q for period t
$H_{q,t}^{com}$	Horsepower consumption of compressor q for period t
$\tau_{q,t}^{com}$	Gas consumption of compressor q's gas turbine for period t
$R_{q,t}^{com}$	Compression ratio of compressor q for period t
$\pi_{n,t}$	Pressure of node n for period t
$I_{i,t}^w$	Working gas inventory of SNGT i for period t
$Q_{i,t}^{inj}, Q_{i,t}^{wdr}$	Injection, withdrawal rates of SNGT i for period t
P_t^m	Power loss of $N-1$ generator outage m
$C_{i,m,t}^g, C_{j,m,t}^c$	Responsive SR of GG i and CG j after $N-1$ outage m for period t
$Pl_{k,t}^{m0}, Pl_{k,t}^m$	Power flow without and with uncertainties after $N-1$ outage m of transmission line k for period t

Parameters

$L_{b,t}^e$	Forecast electricity load at bus b for period t
$P_{s,t}^r$	Forecast power of renewable resource s for period t
$L_{n,t}^{g0}$	Forecast gas load at node n for period t
$P_{i\,\max}^g, P_{i\,\min}^g$	Max, min output of GG i
$P_{j\,\max}^c, P_{j\,\min}^c$	Max, min output of CG j
r_i^g, r_j^c	Ramp rates of GG i and CG j

T	Time period of each dispatch interval
T_a, T_r	Respond time requirements of RR and SR
D_t^a, D_t^r	Total RR and SR requirements for period t
$Pl_{k\,\max}, Pl_{k\,\min}$	Max, min power flow of transmission line k
$\pi_{n\,\max}, \pi_{n\,\min}$	Max, min pressures of node n
$S_{u\,\max}, S_{u\,\min}$	Max, min output of gas supplier u
$Fl_{p\,\max}, Fl_{p\,\min}$	Max, min gas flow of pipeline p
$F_{q\,\max}^{com}, F_{q\,\min}^{com}$	Max, min gas flow of compressor q
$R_{q\,\max}^{com}, R_{q\,\min}^{com}$	Max, min compression ratios of compressor q
$I_{i\,\max}^w, I_{i\,\min}^w$	Max, min inventories of SNGT i
$Q_{i\,\max}^{inj}, Q_{i\,\max}^{wdr}$	Max injection, withdrawal rates of SNGT i
GHV	Natural gas gross heating value, 1015

I. INTRODUCTION

ENERGY crisis, carbon emission and environment pollution have become global challenges. It is an effective solution to strengthen interactions of multiple energy systems, such as electricity, heat and fuels, which envisions a future energy system, called Energy Internet (EI) [1] or Integrated Energy System [2]. With the aim of realizing large-scale renewable integration and improving energy efficiency, EI has aroused a wide concern from government, industry and academia. In China, the State Council has released a series of guiding opinions on actively promoting EI action and emphasized that EI is crucial for promoting energy production and consumption revolutions, optimizing energy utilization structure and supporting healthy and sustainable social development [3]. Moreover, 55 demonstration projects of EI have been approved by National Energy Administration of China in 2017, driving a potential investment over 40 billion Yuan (approximately 6.3 billion dollars).

The fundamental architecture of EI is multi-energy coupled network. Inherently, for electricity, long-distance transmission is mainly adopted because large-scale storage is currently uneconomical; for natural gas, long-distance transportation and large-scale storage are both available; for heat, short-distance transmission is allowed and large capacity storage has been increasingly applied [4]. According to various energy features, the transmission structure of EI is generally composed of electricity and natural gas networks whereas the distribution structure of EI is composed of electricity, natural gas and heat networks. This paper is focused on integrated electricity and natural gas system (IEGS), the transmission layer of EI.

IEGS has been studied in several researches, especially for unified power and gas flow, expansion planning and optimal dispatch problems. Natural gas flow was effectively solved by electrical power flow techniques such as Newton-Raphson method, so that the network analysis for IEGS can be performed in a consistent manner [5]. In [6]–[8], the unified gas and power flow for IEGS was developed from steady-state to probabilistic analysis. Another concerned issue for IEGS is planning, to determine future deployment of electricity and natural gas infrastructures with a least investment. [9]–[11] presented multi-area, multi-stage, multi-load, multi-objective supply/interconnections expansion planning of IEGS.

Moreover, operational technique of IEGS is discussed intensively at day-ahead and real-time horizons. [12] focused on the solution methodology for short-term security-constrained unit commitment of IEGS and a Benders decomposition method was applied. With power-to-gas (P2G) progress, [13] developed an optimal day-ahead scheduling of P2G energy storage and gas load management in wholesale electricity and gas markets. Stochastic day-ahead scheduling of IEGS was presented in [14]–[16] with various uncertainties, including variability of wind energy, random outages of generating units and transmission lines, and forecast errors of day-ahead hourly electricity load. Reserve is designed as an important ancillary service to withstand system uncertainties [17], and reserve was usually scheduled jointly with energy in the economic dispatch of power system [18]–[20]. Nevertheless, reserve scheduling is neglectful or roughly considered in the aforementioned stochastic optimal dispatch of IEGS. Generally, reserve is categorized as regulation reserve (RR) and spinning reserve (SR) [21] (both referred in this paper), where RR is used to balance the forecast error of load and renewable power and SR responds to address unexpected contingencies. Similar to power system, load fluctuation, renewable uncertainty and generator outages in IEGS can be effectively withstood by RR and SR, raising the necessity of integrating reserve scheduling into day-ahead dispatch of IEGS. With the close coupling like gas-fired generators (GGs), reserve scheduling is influenced by electricity and natural gas networks together.

The day-ahead dispatching of IEGS is mathematically formulated as an optimization model, which is difficultly solved because of nonconvex Weymouth gas flow equation. To address this nonconvexity, three common approaches are intelligence algorithm [10], [11], numerical iteration [12]–[14], and convex relaxation including linear approximation [15], [16], [22], [23] and second-order cone (SOC) relaxation [24]–[28]. The classical and improved genetic algorithms as well as the particle swarm optimization algorithm were applied in [10], [11] to manage the nonlinearity of gas flow through the pipeline. In [12] and [14], the natural gas allocation problem with nonlinear equations was solved by Newton-Raphson substitution method. Newton Trust Region method as a superior iterative technique was used for nonlinear optimization problem in [13].

Due to the simplicity and credibility of linear programming algorithm, linearization methods have been widely employed. In [15], [16], Weymouth equation was converted into a set of linear constraints by using a piecewise linear approximation in a 3-D Euclidean space. [22] proposed a multidimensional piecewise linear approximation method for multicarrier energy system which effectively reduced the maximum relative error to 1.85%. Seven piecewise linear models for gas network optimization were compared theoretically and computationally in [23] and incremental linear method presented the best performance in both dynamic and steady-state conditions. In addition, the accuracy of linear approximation significantly depends on the number of linearized segments.

Besides linear approximation, SOC relaxation as an effective convexification way, has been rapidly developed. In [24], [25], quadratic gas flow equations were relaxed into SOC constraints

and second-order cone programming (SOCP) was employed in the distribution network of IEGS where gas flow directions were fixed. However, the assumption of fixed gas flow directions is improper to all IEGSs, especially for transmission networks. Considering unknown gas flow directions, a SOC relaxation of Weymouth equation was proposed in [26] for the expansion planning of gas network and further applied in IEGS operation [27], [28]. Moreover, sequential SOCP methods were investigated in [25] and [28] for optimal gas-power flow calculation to guarantee the tightness of SOC relaxation.

Convex relaxation is a simple and effective method to solve the nonconvex and nonlinear gas flow equations, but it is hard to ensure the feasibility and exactness of optimal solutions. In the previous researches, to provide a more accurate solution, the computational efficiency of both linear approximation and SOC relaxation methods is dramatically reduced. For example, the calculation time of sequential SOCP in [28] was 4–5 times longer than the conventional SOCP, so existing sequential SOCP methods were applied to solve the optimal energy flow at a single period. Thus, it is a great challenge to simultaneously satisfy solution precision and computational efficiency for the multi-period coupled optimization of IEGS, such as day-ahead economic dispatch.

This paper presents a robust day-ahead economic dispatch model for IEGS considering reserve scheduling and various uncertainties including electricity load fluctuation, renewable randomness as well as $N-1$ contingencies. The nonconvexity of the proposed model is addressed by a novel SOC relaxation of Weymouth equation and according to [29], [30], the bi-level robust problem is equivalently reformulated into a single model. Hence, the original robust nonconvex quadratic programming problem is mathematically transformed into a standard mixed integer second-order cone programming (MISOCP) model. Due to the untight relaxation, optimal solutions obtained from MISOCP model are inexact and a gas flow correction method based on Newton-Raphson algorithm is accordingly proposed. The main contributions of this paper are presented as follows:

- Integrate reserve scheduling into day-ahead dispatch of IEGS and achieve the co-optimization of energy and reserve. In previous works, reserve scheduling drew little attention. With the important role of reserve on secure operation, the proposed model considers detailed reserve constraints where RR responds to stochastic load and renewable power and SR is deployed based on $N-1$ criterion. Moreover, the joint dispatch of energy and reserve is widely used in electricity market such as [21] and [29], so the proposed model can be further applied in coordinated gas and electricity market.
- Present a novel SOC relaxation of Weymouth equation considering unfixed gas flow directions. Compared with [26], the major improvement of the proposed SOC relaxation is that squared nodal pressures as decision variables in previous SOC relaxation are replaced by nodal pressures, which presents two advantages: first, due to smaller value range of pressure variables, the feasible region of optimization model is effectively narrowed, beneficial for

reducing computation burden; second, SOC relaxation with pressure variables has a wider application, for example, to manage line pack which is proportional to nodal pressures [31].
- Propose a natural gas flow correction method based on the multi-slack-node gas flow calculation with Newton-Raphson algorithm to ensure the solution accuracy. Sequential SOCP methods in [25] and [28] can realize the tight SOC relaxation, but each iteration needs to solve a MISOCP problem, leading to a lower computational efficiency. The proposed method focuses on directly correcting the gas flow results obtained from MISOCP model and provides the feasible dispatch solution with an evidently shorter computational time.

The rest of paper is organized as following: Section II presents the robust day-ahead dispatch modeling for IEGS; Section III proposes the solution methodology of MISOCP reformulation and gas flow correction; in Section IV, numerical cases are performed on two test IEGSs to demonstrate the effectiveness of the proposed model and approach; finally, conclusions are drawn in Section V.

II. ROBUST DAY-AHEAD DISPATCH MODELLING FOR IEGS

Considering load deviation, renewable unpredictability and $N-1$ outages, a robust day-ahead dispatch model of IEGS is presented in this section.

A. Objective Function

The objective (1) of the day-ahead dispatch model is to minimize the total energy and reserve cost for a whole day. With the assumption of free renewable energy, only coal-fired electricity and natural gas for power, RR and SR are purchased.

$$\min \sum_{t=1}^{N_t} \left(\sum_{u=1}^{N_{sp}} \alpha_{u,t} S_{u,t} + \sum_{j=1}^{N_c} \beta_{j,t}^p P_{j,t}^c + \beta_{j,t}^a A_{j,t}^c + \beta_{j,t}^r R_{j,t}^c \right) T \tag{1}$$

where $\alpha_{u,t}$ is the gas cost coefficient of gas supplier u for period t, $\beta_{j,t}^p, \beta_{j,t}^a, \beta_{j,t}^r$ denote the cost coefficients of power, RR and SR by CG j for period t, respectively.

B. Electricity Network Constraints

The electricity load of IEGS is satisfied by gas-fired, coal-fired and renewable power as (2). The scheduled power, RR and SR are limited by the capacity of GGs and CGs as (3)–(4). The generator ramp constraints between two contiguous dispatch periods and reserve respond time constraints are presented as (5)–(7). Total RR and SR are necessary to meet the reserve capacity requirements in (8). Actually, RR and SR are both active power reserve and day-ahead economic dispatch mainly focuses on the optimal scheduling of active power, so DC power flow is adopted for simplicity. The basic power flow and capacity

limits of transmission lines are formulated as (9).

$$\sum_{i=1}^{N_g} P_{i,t}^g + \sum_{j=1}^{N_c} P_{j,t}^c + \sum_{s=1}^{N_r} P_{s,t}^r = \sum_{b=1}^{N_b} L_{b,t}^e, \forall t \tag{2}$$

$$P_{i,t}^g + A_{i,t}^g + R_{i,t}^g \le P_{i\,\max}^g, P_{i,t}^g - A_{i,t}^g \ge P_{i\,\min}^g, \forall i, t \tag{3}$$

$$P_{j,t}^c + A_{j,t}^c + R_{j,t}^c \le P_{j\,\max}^c, P_{j,t}^c - A_{j,t}^c \ge P_{j\,\min}^c, \forall j, t \tag{4}$$

$$-r_i^g T \le P_{i,t}^g - P_{i,t-1}^g \le r_i^g T, -r_j^c T$$
$$\le P_{j,t}^c - P_{j,t-1}^c \le r_j^c T, \forall i, j, t \tag{5}$$

$$0 \le A_{i,t}^g \le r_i^g T_a, 0 \le R_{i,t}^g \le r_i^g T_r, \forall i, t \tag{6}$$

$$0 \le A_{j,t}^c \le r_j^c T_a, 0 \le R_{j,t}^c \le r_j^c T_r, \forall j, t \tag{7}$$

$$\sum_{i=1}^{N_g} A_{i,t}^g + \sum_{j=1}^{N_c} A_{j,t}^c \ge D_t^a, \sum_{i=1}^{N_g} R_{i,t}^g + \sum_{j=1}^{N_c} R_{j,t}^c \ge D_t^r, \forall t \tag{8}$$

$$\begin{cases} Pl_{k,t}^0 = \sum_{b=1}^{N_b} H_{kb} \left(\sum_{i=1}^{N_g} v_{bi}^g P_{i,t}^g \right. \\ \left. + \sum_{j=1}^{N_c} v_{bj}^c P_{j,t}^c + \sum_{s=1}^{N_r} v_{bs}^r P_{s,t}^r - L_{b,t}^e \right), \forall k, t \\ Pl_{k\,\min} \le Pl_{k,t}^0 \le Pl_{k\,\max} \end{cases} \tag{9}$$

where H_{kb} is the element of power transmission distribution factor (PTDF) matrix, v_{bi}^g is the element of GG-bus incidence matrix, if GG i is located at bus b, $v_{bi}^g = 1$, else $v_{bi}^g = 0$, similarly v_{bj}^c is the element of CG-bus incidence matrix, v_{bs}^r is the element of renewable resource-bus incidence matrix.

The uncertainties of electricity load and renewable power are managed jointly as a series of stochastic forecast errors $E_{b,t}$ at each bus within the interval $[E_{b,t}^{\min}, E_{b,t}^{\max}]$ where the upper and lower bounds are relative to the forecast electricity load and renewable power in (10). Scheduled RR of each electricity bus is unfixed and optimally allocated as (11)–(12) by the use of participation factors to withstand the total forecast error of electricity load and renewable power.

$$E_{b,t}^{\max} = \delta_r \sum_{s=1}^{N_r} v_{bs}^r P_{s,t}^r + \delta_e L_{b,t}^e, E_{b,t}^{\min} = -E_{b,t}^{\max}, \forall b, t \tag{10}$$

$$\sum_{b=1}^{N_b} \lambda_{b,t} = 1, 0 \le \lambda_{b,t} \le 1, \forall b, t \tag{11}$$

$$-\sum_{i=1}^{N_g} v_{bi}^g A_{i,t}^g - \sum_{j=1}^{N_c} v_{bj}^c A_{j,t}^c \le \lambda_{b,t} \sum_{b=1}^{N_b} E_{b,t} \le \sum_{i=1}^{N_g} v_{bi}^g A_{i,t}^g$$
$$+ \sum_{j=1}^{N_c} v_{bj}^c A_{j,t}^c, \forall E_{b,t} \in [E_{b,t}^{\min}, E_{b,t}^{\max}], b, t \tag{12}$$

where δ_e, δ_r denote the fixed proportion of forecast electricity load and renewable power respectively, which reflect the forecast error confidence interval [30], $\lambda_{b,t}$ is the participation factor of generators at bus b for period t to provide RR which is treated as a variable. With the load and renewable uncertainties, the power flow of transmission lines is accordingly stochastic, and

the robust form of constraint (9) is formulated as (13).

$$\begin{cases} Pl_{k,t} = \sum_{b=1}^{N_b} H_{kb} \\ \left(\sum_{i=1}^{N_g} v_{bi}^g P_{i,t}^g + \sum_{j=1}^{N_c} v_{bj}^c P_{j,t}^c + \sum_{s=1}^{N_r} v_{bs}^r P_{s,t}^r - L_{b,t}^e \right) \\ + \sum_{b=1}^{N_b} H_{kb} \left(-E_{b,t} + \lambda_{b,t} \sum_{b=1}^{N_b} E_{b,t} \right) \\ = Pl_{k,t}^0 + \sum_{b=1}^{N_b} H_{kb} \left(-E_{b,t} + \lambda_{b,t} \sum_{b=1}^{N_b} E_{b,t} \right) \\ Pl_{k\,\min} \le Pl_{k,t} \le Pl_{k\,\max} \end{cases}$$
$$, \forall E_{b,t} \in [E_{b,t}^{\min}, E_{b,t}^{\max}], k, t \tag{13}$$

Since the renewable forecast error is described by an interval with fixed proportion, it is unnecessary to emphasize the stochastic characteristics of different renewable infrastructures.

C. Natural Gas Network Constraints

The nodal natural gas balance equation is presented in (14). The supplier output and nodal pressures are limited as (15)–(16). The steady-state gas transportation constraints are formulated as (17)–(19) with Weymouth equation. In the studied IEGS, all compressors are gas-powered. Horsepower consumption of the compressor is determined by (20). The relation of gas and horsepower consumption for a compressor is approximate to linearity in (21). The inlet and outlet pressures are limited by the extreme compression ratio in (22) and transported gas of a compressor is restricted in (23).

$$\sum_{u=1}^{N_{sp}} v_{nu}^{sp} S_{u,t} - L_{n,t}^g = \sum_{p=1}^{N_f} v_{np}^f Fl_{p,t} + \sum_{q=1}^{N_{com}} v_{nq}^c F_{q,t}^{com}$$
$$+ \sum_{q=1}^{N_{com}} v_{nq}^{ct} \tau_{q,t}^{com}, \forall n, t \tag{14}$$

$$S_{u\,\min} \le S_{u,t} \le S_{u\,\max}, \forall u, t \tag{15}$$

$$\pi_{n\,\min} \le \pi_{n,t} \le \pi_{n\,\max}, \forall n, t \tag{16}$$

$$Fl_{p,t} = \text{sgn}(n,l)_{p,t} c_p \sqrt{|\pi_{n,t}^2 - \pi_{l,t}^2|}, \forall p, t \tag{17}$$

$$\text{sgn}(n,l)_{p,t} = \begin{cases} +1, & (\pi_{n,t} - \pi_{l,t}) \ge 0 \\ -1, & (\pi_{n,t} - \pi_{l,t}) < 0 \end{cases}, \forall p, t \tag{18}$$

$$Fl_{p\,\min} \le Fl_{p,t} \le Fl_{p\,\max}, \forall p, t \tag{19}$$

$$H_{q,t}^{com} = B_q F_{q,t}^{com} \left[\left(\frac{\pi_n}{\pi_{l'}} \right)^{Z_q} - 1 \right], \forall q, t \tag{20}$$

$$GHV \cdot \tau_{q,t}^{com} = b_q^{com} H_{q,t}^{com}, \forall q, t \tag{21}$$

$$\begin{cases} \pi_{l',t} = R_{q,t}^{com} \pi_{n,t} \\ R_{q\,\min}^{com} \le R_{q,t}^{com} \le R_{q\,\max}^{com} \end{cases}, \forall q, t \tag{22}$$

$$F_{q\,\min}^{com} \le F_{q,t}^{com} \le F_{q\,\max}^{com}, \forall q, t \tag{23}$$

where v_{nu}^{sp} is the element of gas supplier-node incidence matrix, v_{np}^f is the element of pipeline-node incidence matrix, v_{nq}^c is the element of compressor-node incidence matrix, v_{nq}^{ct} is the element of compressor's gas turbine-node incidence matrix, c_p

denotes Weymouth constant of pipeline p (from node n to l), B_q, Z_q are horsepower consumption constants of compressor q (from node n to l'), b_q^{com} is energy conversion coefficient of horsepower to gas consumption for compressor q's gas turbine.

D. Coupling Constraints of Electricity and Gas Networks

The electricity and natural gas networks are mainly interconnected by GGs in the studied IEGS. The GG is an energy supplier for electricity network whereas an energy consumer for gas network. The power-gas curve of a GG can be described by a linear function as (24). Similarly, the gas consumption of scheduled RR and SR are formulated as (25). To prestore adequate gas for providing reserve, self-owned natural gas tanks (SNGTs) of GGs are deployed fully used for gas-fired RR and SR so that constraints of SNGTs are formulated as (26)–(29). The working gas inventory is balanced between two contiguous dispatch periods as (26) with the limitation of storage capacity in (27). Considering the worst condition that scheduled gas reserve for each interval is all consumed, the injection and withdrawal rates of SNGTs are limited as (28). Besides, the working gas inventory is desired to be balanced by the end of day-ahead dispatch as (29).

$$GHV \cdot G_{i,t}^p = b_i^g P_{i,t}^g, \forall i,t \tag{24}$$

$$GHV \cdot G_{i,t}^a = b_i^g A_{i,t}^g, GHV \cdot G_{i,t}^r = b_i^g R_{i,t}^g, \forall i,t \tag{25}$$

$$I_{i,t}^w = I_{i,t-1}^w + (Q_{i,t}^{inj} - Q_{i,t}^{wdr})T, \forall i,t \tag{26}$$

$$I_{i\,\min}^w \le I_{i,t}^w \le I_{i\,\max}^w, \forall i,t \tag{27}$$

$$\begin{cases} 0 \le Q_{i,t}^{inj} \le Q_{i\,\max}^{inj} \\ 0 \le Q_{i,t}^{wdr} = G_{i,t}^a + G_{i,t}^r \le Q_{i\,\max}^{wdr} \end{cases}, \forall i,t \tag{28}$$

$$I_{i,0}^w = I_{i,N_t}^w, \forall i \tag{29}$$

where b_i^g denotes the heat rate coefficient of GG i.

With the coupling of GGs, natural gas load is updated as (30). The increase of gas load in (30) is derived from natural gas demand for gas-fired power and reserve.

$$L_{n,t}^g = L_{n,t}^{g0} + \sum_{i=1}^{N_g} v_{ni}^{gn}(G_{i,t}^p + Q_{i,t}^{inj}), \forall n,t \tag{30}$$

where v_{ni}^{gn} is the element of GG-node incidence matrix.

E. $N-1$ Generator Outage Constraints

In order to ensure the security and reliability of IEGS operation, $N-1$ criterion is fundamental to be satisfied, especially $N-1$ generator outages which can be effectively addressed by scheduling SR. Once $N-1$ outage m of CGs or GGs occurs, SR responds to withstand the power loss as (31). The responsive SR is restricted by (32) and inevitably leads to the redispatch of power flow. Similar to (13), considering the randomness of electricity load and renewable power, the power flow after $N-1$ generator outage is robustly formulated as (33) with the transmission capacity limitation. With the above assumption of

gas storage utilization, responsive SR of GGs is fully produced from the gas of SNGTs, resulting in the gas flow unchanged after $N-1$ generator outages. Moreover, considering the long time constant of natural gas transportation, the gas load change is not involved in this day-ahead dispatch.

$$\sum_{i=1,i\neq m}^{N_g} C_{i,m,t}^g + \sum_{j=1,j\neq m}^{N_c} C_{j,m,t}^c = P_t^m, \forall m,t \tag{31}$$

$$\begin{cases} 0 \le C_{i,m,t}^g \le R_i^g, \forall i \neq m \\ 0 \le C_{j,m,t}^c \le R_j^c, \forall j \neq m \end{cases} \tag{32}$$

$$\begin{cases} Pl_{k,t}^m = \sum_{b=1}^{N_b} H_{kb} \Big[\sum_{i=1,i\neq m}^{N_g} v_{bi}^g (P_{i,t}^g + C_{i,m,t}^g) \\ \quad + \sum_{j=1,j\neq m}^{N_c} v_{bj}^c (P_{j,t}^c + C_{j,m,t}^c) \\ \quad + \sum_{s=1}^{N_r} v_{bs}^r P_{s,t}^r - L_{b,t}^e \Big] \\ \quad + \sum_{b=1}^{N_b} H_{kb} \Big(-E_{b,t} + \lambda_{b,t} \sum_{b=1}^{N_b} E_{b,t} \Big) \\ \quad = Pl_{k,t}^{m0} + \sum_{b=1}^{N_b} H_{kb} \Big(-E_{b,t} + \lambda_{b,t} \sum_{b=1}^{N_b} E_{b,t} \Big) \\ Pl_{k\,\min}^m \le Pl_{k,t}^m \le Pl_{k\,\max}^m, \end{cases}$$

$$\forall E_{b,t} \in [E_{b,t}^{\min}, E_{b,t}^{\max}], m,k,t \tag{33}$$

III. SOLUTION METHODOLOGY

The above day-ahead dispatch model is a robust nonconvex problem. To make it solvable, a novel SOC relaxation is presented in this section and the original model is converted into a typical MISOCP. Then a gas flow correction method is proposed to ensure the exactness of dispatch solutions.

A. Relaxation of Nonconvex Gas Network Constraints

The Weymouth equation introduced in (17)–(18) is the major nonconvex performance of IEGS. Based on Big M approach, constraints (17)–(18) are reformulated as (34)–(36) with the new introduced binary integers instead of the sign function.

$$x_{p,t}(1 - x_{p,t}) = 0, \forall p,t \tag{34}$$

$$\begin{cases} -Mx_{p,t} \le \pi_{n,t} - \pi_{l,t} \le M(1 - x_{p,t}) \\ -Mx_{p,t} \le Fl_{p,t} \le M(1 - x_{p,t}) \end{cases}, \forall p,t \tag{35}$$

$$Fl_{p,t}^2 = (1 - 2x_{p,t})c_p^2(\pi_{n,t}^2 - \pi_{l,t}^2), \quad \forall p,t \tag{36}$$

where $x_{p,t}$ is an introduced 0–1 integer variable of pipeline p for period t to represent the gas flow direction.

Evidently, the quadratic equalities of (36) possess the nonconvex properties. To obtain the convex feasible region, the constraints (36) are conically relaxed into inequalities as (37). With the use of 0–1 variables, constraint (37) is reformulated as a piecewise inequality (38), which is equivalent to the piecewise

SOC constraint as (39).

$$Fl_{p,t}^2 \le (1 - 2x_{p,t})c_p^2(\pi_{n,t}^2 - \pi_{l,t}^2), \forall p, t \qquad (37)$$

$$Fl_{p,t}^2 \le \begin{cases} c_p^2(\pi_{n,t}^2 - \pi_{l,t}^2), & x_{p,t} = 0 \\ c_p^2(\pi_{l,t}^2 - \pi_{n,t}^2), & x_{p,t} = 1 \end{cases}, \forall p, t \qquad (38)$$

$$\begin{cases} \left\| \begin{matrix} Fl_{p,t} \\ c_p \pi_{l,t} \end{matrix} \right\|_2 \le c_p \pi_{n,t}, & x_{p,t} = 0 \\ \left\| \begin{matrix} Fl_{p,t} \\ c_p \pi_{n,t} \end{matrix} \right\|_2 \le c_p \pi_{l,t}, & x_{p,t} = 1 \end{cases}, \forall p, t \qquad (39)$$

Constraint (39) is further developed into a single formulation with two continuous variables introduced as (40), which can be reformulated into linear constraints (41)–(42) with big M value. Thus, a standard SOC relaxation of Weymouth equation is presented as (43) to eliminate the nonconvexity.

$$u_{p,t} = \begin{cases} \pi_{n,t}, x_{p,t} = 0 \\ \pi_{l,t}, x_{p,t} = 1 \end{cases}, v_{p,t} = \begin{cases} \pi_{l,t}, x_{p,t} = 0 \\ \pi_{n,t}, x_{p,t} = 1 \end{cases}, \forall p, t \qquad (40)$$

$$\begin{cases} -\mathrm{M}x_{p,t} \le u_{p,t} - \pi_{n,t} \le \mathrm{M}x_{p,t} \\ -\mathrm{M}(1 - x_{p,t}) \le u_{p,t} - \pi_{l,t} \le \mathrm{M}(1 - x_{p,t}) \end{cases}, \forall p, t \qquad (41)$$

$$\begin{cases} -\mathrm{M}x_{p,t} \le v_{p,t} - \pi_{l,t} \le \mathrm{M}x_{p,t} \\ -\mathrm{M}(1 - x_{p,t}) \le v_{p,t} - \pi_{n,t} \le \mathrm{M}(1 - x_{p,t}) \end{cases}, \forall p, t \qquad (42)$$

$$\left\| \begin{matrix} Fl_{p,t} \\ c_p v_{p,t} \end{matrix} \right\|_2 \le c_p u_{p,t}, \qquad \forall p, t \qquad (43)$$

Another nonconvex constraint is derived from horsepower consumption of compressors as (20). The gas consumption of a compressor is typically 3~5% of the transported gas [32], which has little impact on natural gas dispatching. Thus, constraint (44) is a common approximation of complex equalities (20)–(21).

$$\begin{cases} \tau_{q,t}^{com} = \eta_{q,t}^{com} F_{q,t}^{com} \\ \eta_{q,t}^{com} = 3\% \sim 5\% \end{cases}, \forall q, t \qquad (44)$$

Hence, the nonconvexity of day-ahead dispatch model for IEGS is addressed by the SOC relaxation of Weymouth gas flow equation and linear simplification of higher-order compressor consumption constraints.

B. Reformulation of Robust Optimization Model

Actually, the robust programming is to seek a feasible optimal solution which is able to satisfy all the constraints for any given realization within the uncertainty set [29], such as the interval $[E_{b,t}^{\min}, E_{b,t}^{\max}]$. The robust formulations of (12) and (13) are equivalent to the constraints (45)–(46) with the use of the worst-case approach. Therefore, the original robust model is a bi-level

optimization problem.

$$\begin{cases} \max_{E_{b,t}^{\min} \le E_{b,t} \le E_{b,t}^{\max}} \lambda_{b,t} \sum_{b=1}^{N_b} E_{b,t} \le \sum_{i=1}^{N_g} v_{bi}^g A_{i,t}^g \\ + \sum_{j=1}^{N_c} v_{bj}^c A_{j,t}^c \\ \min_{E_{b,t}^{\min} \le E_{b,t} \le E_{b,t}^{\max}} \lambda_{b,t} \sum_{b=1}^{N_b} E_{b,t} \ge -\sum_{i=1}^{N_g} v_{bi}^g A_{i,t}^g \\ - \sum_{j=1}^{N_c} v_{bj}^c A_{j,t}^c \end{cases}, \forall b, t \qquad (45)$$

$$\begin{cases} \max_{E_{b,t}^{\min} \le E_{b,t} \le E_{b,t}^{\max}} Pl_{k,t}^0 \\ + \sum_{b=1}^{N_b} H_{kb} \left(-E_{b,t} + \lambda_{b,t} \sum_{b=1}^{N_b} E_{b,t} \right) \le Pl_{k\max} \\ \min_{E_{b,t}^{\min} \le E_{b,t} \le E_{b,t}^{\max}} Pl_{k,t}^0 \\ + \sum_{b=1}^{N_b} H_{kb} \left(-E_{b,t} + \lambda_{b,t} \sum_{b=1}^{N_b} E_{b,t} \right) \ge Pl_{k\min} \end{cases}, \forall k, t \qquad (46)$$

According to [30], the constraint (45) is reformulated as (47) mathematically, which achieves the simplification of bi-level robust model.

$$\begin{cases} y_{1b,t} \sum_{b=1}^{N_b} E_{b,t}^{\max} + y_{2b,t} \sum_{b=1}^{N_b} E_{b,t}^{\min} \le \sum_{i=1}^{N_g} v_{bi}^g A_{i,t}^g \\ + \sum_{j=1}^{N_c} v_{bj}^c A_{j,t}^c \\ y_{1b,t} \sum_{b=1}^{N_b} E_{b,t}^{\min} + y_{2b,t} \sum_{b=1}^{N_b} E_{b,t}^{\max} \\ \ge -\sum_{i=1}^{N_g} v_{bi}^g A_{i,t}^g - \sum_{j=1}^{N_c} v_{bj}^c A_{j,t}^c \\ y_{1b,t} \ge 0, y_{1b,t} \ge \lambda_{b,t} \\ y_{2b,t} \le 0, y_{2b,t} \le \lambda_{b,t} \end{cases}, \forall b, t \qquad (47)$$

with dummy variables $y_{1b,t}$ and $y_{2b,t}$.

Similarly, the constraint (46) of power flow can be transformed into (48). The reformulation of robust power flow with $N-1$ outages in (33) is similar to (13). Hence, the bi-level formulation of robust programming is equivalently transformed into a solvable single model with the introduced dummy continuous variables.

$$\begin{cases} Pl_{k,t}^0 + \sum_{b=1}^{N_b} z_{1kb,t} E_{b,t}^{\max} + \sum_{b=1}^{N_b} z_{2kb,t} E_{b,t}^{\min} \\ \le Pl_{k\max}, \forall k, t \\ Pl_{k,t}^0 + \sum_{b=1}^{N_b} z_{1kb,t} E_{b,t}^{\min} + \sum_{b=1}^{N_b} z_{2kb,t} E_{b,t}^{\max} \\ \ge Pl_{k\min}, \forall k, t \\ z_{1kb,t} \ge 0, z_{1kb,t} \ge -H_{kb} + \sum_{b=1}^{N_b} H_{kb}\lambda_{b,t}, \forall k, b, t \\ z_{2kb,t} \le 0, z_{2kb,t} \le -H_{kb} + \sum_{b=1}^{N_b} H_{kb}\lambda_{b,t}, \forall k, b, t \end{cases} \qquad (48)$$

with dummy variables $z_{1kb,t}$ and $z_{2kb,t}$.

C. Gas Flow Correction for Exact IEGS Dispatch

The original robust nonconvex day-ahead dispatch model of IEGS is creditably reformulated into a standard MISOCP model, which is solved to provide the optimal solutions of electricity and natural gas networks. Nevertheless, especially for a loop

network, SOC relaxation of Weymouth equation fails to provide the exact gas flow solution, which is indispensable for IEGS operation, such as day-ahead dispatch. Accordingly, gas flow correction after solving MISOCP model is necessary.

Intuitively, inexact gas flow solution can be corrected by the multi-slack-node gas flow model with Newton-Raphson method in [8]. Gas flow equations are formulated as (49), according to constraints (14), (17), (44) and (22). Each gas supplier is regarded as a slack node, and consequently, the gas output of suppliers is revised by (50).

$$\begin{cases} \Delta L_{n,t} = \sum_{u=1}^{N_{sp}} v_{nu}^{sp} S_{u,t} - L_{n,t}^g - \sum_{p=1}^{N_f} v_{np}^f Fl_{p,t} \\ \quad - \sum_{q=1}^{N_{com}} v_{nq}^c F_{q,t}^{com} - \sum_{q=1}^{N_{com}} v_{nq}^{ct} \tau_{q,t}^{com} = 0, \forall n,t \\ \Delta Fl_{p,t} = Fl_{p,t}|Fl_{p,t}| - c_p\left(\pi_{n,t}^2 - \pi_{l,t}^2\right) = 0, \forall p,t \\ \Delta \tau_{q,t}^{com} = \tau_{q,t}^{com} - \eta_{q,t}^{com} F_{q,t}^{com} = 0, \forall q,t \\ \Delta \pi_{q,t} = \pi_{l',t} - R_{q,t}^{com}\pi_{n,t} = 0, \forall q,t \end{cases} \quad (49)$$

$$\begin{cases} S_{u,t} = S_{u,t}^0 + \theta_u \Delta S_t \\ \theta_u = S_{u\max} \Big/ \sum_{u=1}^{N_{sp}} S_{u\max} \end{cases}, \forall u,t \quad (50)$$

where $\Delta L_{n,t}$ is the gas injection unbalance at node n for period t, $\Delta Fl_{p,t}$ is the gas flow unbalance of pipeline p for period t, $\Delta \tau_{q,t}^{com}$ is the gas consumption unbalance of compressor q for period t, $\Delta \pi_{q,t}$ is the pressure unbalance of compressor q for period t, $S_{u,t}^0$ is the initial output of gas supplier u for period t, ΔS_t is the total gas output unbalance for period t, θ_u is a fixed participation factor of gas supplier u.

Denote Y_t to the unbalance vector, X_t to the state vector as (51) where $\Delta L_t, \Delta Fl_t, \Delta \tau_t, \Delta \pi_t, Fl_t, F_t^{com}, \tau_t^{com}$ are vectors of all $\Delta L_{n,t}, \Delta Fl_{p,t}, \Delta \tau_{q,t}^{com}, \Delta \pi_{q,t}, Fl_{p,t}, F_{q,t}^{com}, \tau_{q,t}^{com}$ and π_t is the vector of all $\pi_{n,t}$ excluding the pressure of reference node. The first order Taylor expansion of (49) with respect to X_t^{z-1} from the last iteration is formulated as (52) with the Jacobi Matrix in (53).

$$Y_t = [\Delta L_t; \Delta Fl_t; \Delta \tau_t; \Delta \pi_t], X_t$$
$$= [\pi_t; Fl_t; F_t^{com}; \tau_t^{com}; \Delta S_t], \forall t \quad (51)$$

$$Y_t^z = Y_t^{z-1} + J(X_t^{z-1})(X_t^z - X_t^{z-1}) = 0, \forall t \quad (52)$$

$$J = \begin{bmatrix} 0 & \frac{\partial \Delta L_t}{\partial Fl_t} & \frac{\partial \Delta L_t}{\partial F_t^{com}} & \frac{\partial \Delta L_t}{\partial \tau_t^{com}} & \frac{\partial \Delta L_t}{\partial \Delta S_t} \\ \frac{\partial \Delta Fl_t}{\partial \pi_t} & \frac{\partial \Delta Fl_t}{\partial Fl_t} & 0 & 0 & 0 \\ 0 & 0 & \frac{\partial \Delta \tau_t}{\partial F_t^{com}} & \frac{\partial \Delta \tau_t}{\partial \tau_t^{com}} & 0 \\ \frac{\partial \Delta \pi_t}{\partial \pi_t} & 0 & 0 & 0 & 0 \end{bmatrix}, \forall t \quad (53)$$

For clarity, the procedure of MISOCP reformulation and gas flow correction for exact IEGS day-ahead dispatch solution is presented in Fig. 1. The execution steps of Newton-Raphson gas flow correction are presented as follows.

Step 1: Input the optimal solution of MISOCP model where gas demand of GGs and compression ratios are predefined operating conditions, gas output of suppliers, nodal pressures, gas flow of pipelines and compressors and gas consumption of compressors are
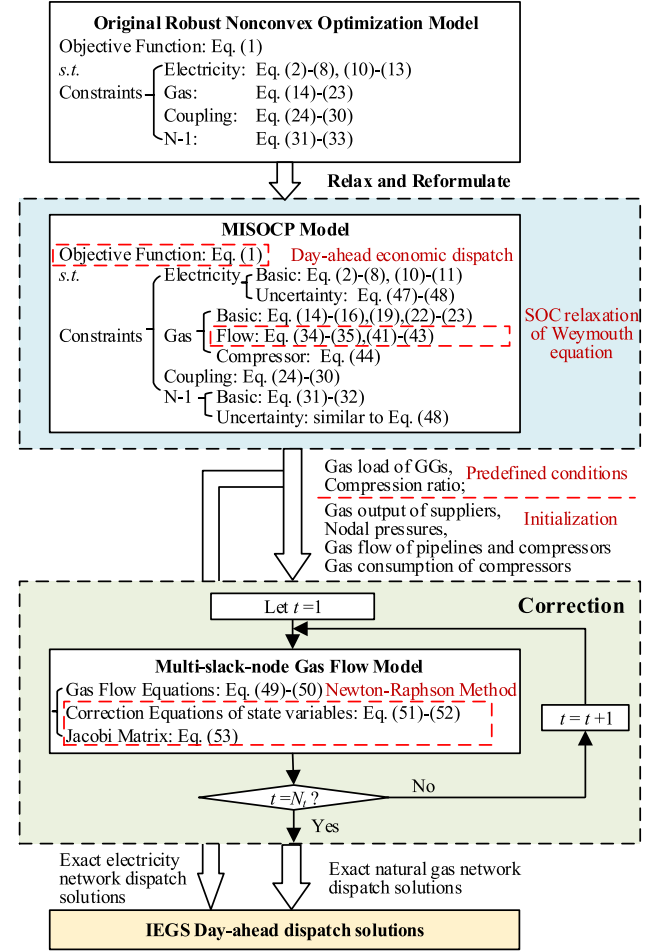

Fig. 1. The procedure of MISOCP reformulation and gas flow correction for exact IEGS day-ahead dispatch.

the initialization of $S_{u,t}^0$ and X_t^0. Set iteration number $z = 0$, initial gas output unbalance $\Delta S_t^0 = 0$, and convergence precision ε.

Step 2: Compute the unbalance vector Y_t^z by (49)–(50). If $\max(Y_t^z) \leq \varepsilon$, stop and output the correctional dispatch results of natural gas network; otherwise, go to step 3.

Step 3: Compute $J(X_t^z)$ by (53), and update the state vector X_t^{z+1} according to $X_t^{z+1} = X_t^z - J^{-1}(X_t^z)Y_t^z$ obtained from (52). Then go back to step 2.

IV. NUMERICAL TESTS

The proposed day-ahead economic dispatch model with solution methodology for IEGS is examined on an IEEE 39-bus-15-node test IEGS and an IEEE 118-bus-40-node test IEGS. The respond time requirements of RR and SR T_a and T_r are 5 min and 10 min, Big M value is 10^6, and convergence precision of Newton-Raphson method is 10^{-6}. The numerical experiments are performed using MATLAB R2013a and CPLEX 12.5 on a personal computer with Intel(R) Core(TM) i7-4790 CPU(3.60 GHz) and 8.00 GB RAM.
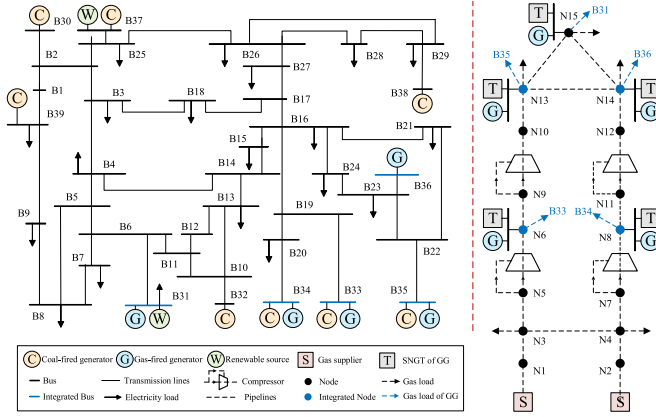
Fig. 2.   Topology of the IEEE 39-bus-15-node test IEGS.

Fig. 3.   Day-ahead forecast electricity load, gas load and renewable power.

TABLE I
DATA OF CGS IN THE IEEE 39-BUS-15-NODE TEST IEGS

Bus	Units	Max output (MW)	Min output (MW)	Ramp (MW/min)	Offering price ($/MWh)		
					Power	RR	SR
30,34	1	500	150	10	18.919	27.28	24.65
32,35,37	2	350	100	7	23.667	28.20	25.70
33	1	600	180	12	15.345	23.06	22.88
38	3	250	80	5	27.924	30.00	26.50
39	2	500	150	10	18.919	27.28	24.65

TABLE II
DATA OF GGS IN THE IEEE 39-BUS-15-NODE TEST IEGS

Bus	Node	Units	Max output (MW)	Min output (MW)	Ramp (MW/min)	Heat rate coefficient (MBtu/MWh)
31	15	2	416	83.2	16.65	11.0150
33	6	1	220	44.0	8.80	14.2920
34	8	1	341	68.2	13.60	13.8400
35	13	1	341	68.2	13.60	13.8400
36	14	2	416	83.2	16.65	11.0150

TABLE III
CASES OF THE IEEE 39-BUS-15-NODE TEST IEGS

Case	Max forecast error $E_{b,t}^{\max}$ (MW)	Gas price ($/MMSCF)		N-1 outage	Pipeline capacity
1	0	Node 1	190	B33 CG	Base
		Node 2	210	B31 GG	
2	3% E-load+5% R-power	Node 1	190	B33 CG	Base
		Node 2	210	B31 GG	
3	5% E-load+10% R-power	Node 1	190	B33 CG	Base
		Node 2	210	B31 GG	
4	3% E-load+5% R-power	Node 1	600	B33 CG	Base
		Node 2	630	B31 GG	
5	3% E-load+5% R-power	Node 1	190	No	Base
		Node 2	210		
6	3% E-load+5% R-power	Node 1	190	B33 CG	1.5 Base
		Node 2	210	B31 GG	

A. IEEE 39-Bus-15-Node Test IEGS

1) Introduction of Test System and Cases: The IEEE 39-bus-15-node test IEGS is presented in Fig. 2, including 8 CGs, 5 GGs with SNGTs, 2 renewable resources, 46 transmission lines, 2 gas suppliers, 12 pipelines, 4 compressors. The data of CGs and GGs is available in Table I and Table II. The renewable resources are located at B31 with 300 MW and B37 with 200 MW. The detailed data of gas network is available in [11]. The hourly forecast electricity load, natural gas load (without demand of GGs) and renewable power are profiled in Fig. 3. The RR capacity requirement is 2% forecast electricity load, and the SR capacity requirement is the larger alternative of 8% forecast electricity load and the max single unit capacity. The gas consumption coefficients of 4 compressors are identically 3%. N1 is the pressure reference node at 1200 Psia, constantly. Besides, the max $N - 1$ outages of CG (unit at B33) and GG (unit at B31) are considered.

To demonstrate the effectiveness of the proposed model and approach for IEGS, several cases are designed as Table III,
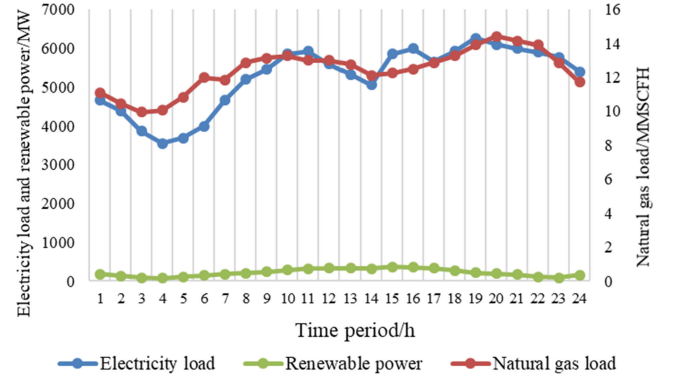
where E-load and R-power refer to the forecast electricity load and renewable power, respectively.

2) Effectiveness of the Proposed MISOCP Model With Gas Flow Correction Method: The proposed MISOCP model is compared with the previous MISOCP model widely used in [26]–[28] as well as MILP model using incremental piecewise linearization available in [23]. The piecewise linear effect is related to the segments, so two MILP models with 10 segments (MILP-1) and 30 segments (MILP-2) are applied. The dispatch interval T is set as 2 h, and the objective and computational efficiency analysis for MISOCP and MILP models with different cases is presented in Table IV where time only refers to the calculation time of optimization model.

According to Table IV, the optimal objective results of two MISOCP models are nearly the same whereas averagely 0.86% lower than MILP-1 and 0.57% lower than MILP-2. Though the declined rate is not high, but the amount of total cost is considerable, especially for a large-scale IEGS or a peak-time price. Moreover, computational time varies intensely for different predefined conditions, and the introduction of uncertainty and $N - 1$ outage constraints is the dominating impact factor to increase the computational time. Compared with the previous MISOCP model, the proposed MISOCP effectively enhances the solution efficiency. The computational efficiency of MILP model is reduced with the increasing linear segments for higher

TABLE IV
OBJECTIVE AND COMPUTATIONAL EFFICIENCY ANALYSIS FOR MISOCP AND MILP MODELS WITH DIFFERENT CASES IN THE IEEE 39-BUS-15-NODE TEST IEGS

Case	Proposed MISOCP				Previous MISOCP				MILP-1			MILP-2		
	Obj (10^6\$)	Time (Sec)	Cones	Integers	Obj (10^6\$)	Time (Sec)	Cones	Integers	Obj (10^6\$)	Time (Sec)	Integers	Obj (10^6\$)	Time (Sec)	Integers
1	2.3244	4.34	144	144	2.3244	7.64	144	144	2.3444	4.90	1296	2.3375	25.37	4176
2	2.3648	22.51	144	144	2.3649	83.78	144	144	2.3845	16.77	1296	2.3783	53.18	4176
3	2.4427	39.73	144	144	2.4427	85.83	144	144	2.4632	28.48	1296	2.4565	56.34	4176
4	2.6629	31.43	144	144	2.6629	71.52	144	144	2.6793	10.05	1296	2.6740	36.74	4176
5	2.3648	11.11	144	144	2.3648	31.07	144	144	2.3845	5.88	1296	2.3783	32.70	4176
6	1.9477	13.90	144	144	1.9478	56.92	144	144	1.9734	2.82	1296	1.9630	16.89	4176

TABLE V
FEASIBILITY OF GAS FLOW CORRECTION METHOD FOR MISOCP MODELS WITH DIFFERENT CASES IN THE IEEE 39-BUS-15-NODE TEST IEGS

Case	Proposed MISOCP			Previous MISOCP		
	Time (Sec)	Maxerr (%)	Average iterations	Time (Sec)	Maxerr (%)	Average iterations
1	0.029	1.3×10^{-5}	4	0.029	1.8×10^{-6}	4
2	0.030	4.6×10^{-9}	4	0.029	1.3×10^{-6}	4
3	0.034	1.3×10^{-7}	4	0.028	4.3×10^{-7}	4
4	0.030	6.6×10^{-5}	4	0.031	1.5×10^{-5}	4
5	0.028	1.7×10^{-6}	4	0.030	1.1×10^{-7}	4
6	0.031	1.2×10^{-7}	5	0.030	5.9×10^{-5}	5

Fig. 4. Hourly coal-fired and gas-fired power and reserve of Case 2 in the IEEE 39-bus-15-node test IEGS.

precision, and the computational time of MILP-2 is longer than the proposed MISOCP for all cases.

Due to different SOC formulations, squared nodal pressures as decision variables in the previous MISOCP are replaced by nodal pressures in the proposed MISOCP, which contributes to two improvements. First, with smaller value range of pressure variables, the feasible region of optimization model is narrowed effectively, resulting in a lighter computation burden. Second, SOC relaxation using pressure variables can be applied in more researches of IEGS. For example, when concerning the line pack which is proportional to pressures at the two end nodes of a pipeline [31], the proposed MISOCP is more practical.

Additionally, a gas flow error is defined as formula (54) to estimate the relaxation effect of Weymouth equation.

$$err_{p,t} = \left| \frac{Fl_{p,t} - \text{sgn}(n,l)_{p,t} c_p \sqrt{|\pi_{n,t}^2 - \pi_{l,t}^2|}}{\text{sgn}(n,l)_{p,t} c_p \sqrt{|\pi_{n,t}^2 - \pi_{l,t}^2|}} \right| \times 100\%, \forall p, t \tag{54}$$

For Case 2, due to the loop gas network, the maximum gas flow errors of the proposed and previous MISOCP models are 13.23% and 17.87%, unqualified for IEGS operation. Therefore, the gas flow correction method is necessarily employed to obtain feasible natural gas network solutions. The convergence property of two MISOCP models is discussed in Table V where maxerr and time refer to the maximum gas flow error obtained by (54) and calculation time of correction procedure, respectively. According to simulation results, all gas flow can be converged rapidly with a satisfactory precision, which illustrates both MISOCP models can provide a good initial point for the gas flow execution. After correction, the scheduled output
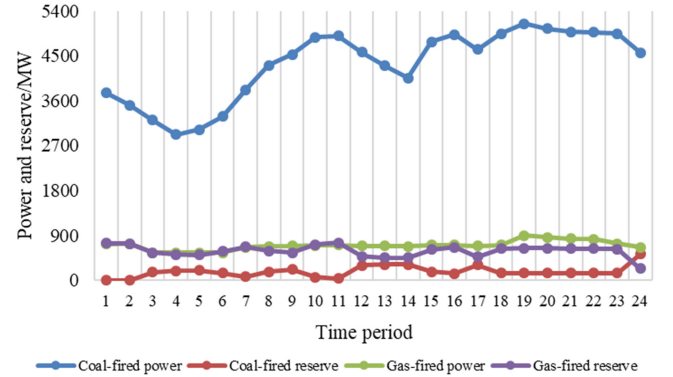
of gas suppliers is not changed as well as the objective value of total cost.

Hence, the proposed MISOCP model provides a more economic dispatch solution with a shorter computational time than MILP model, and presents the superiority in narrower feasible region, higher computational efficiency and wider application than the previous MISOCP model. Furthermore, the proposed gas flow correction method is feasible and effective for both MISOCP models to achieve exact solutions.

3) Day-Ahead Dispatch Results of Test IEGS: Set dispatch interval T as 1 h, and the optimal hourly dispatch results are available based on the proposed MISOCP model and gas flow correction method. The hourly coal-fired and gas-fired power and reserve of Case 2 are scheduled as Fig. 4.

In Case 2, 86% power is provided by CGs for electricity load in the test IEGS, whereas 92% RR and 72% SR are provided by GGs. However, CGs totally supply 78% power and reserve more than the rated capacity proportion (68%), which is discrepant to the perception that cheaper suppliers (GGs) have larger power output. To interpret the unexpected results, the hourly gas flow of pipelines is traced where the maximum gas flow of pipeline N10-N13 and pipeline N12-N14 has already reached the upper bound of transportation capacity. Hence, the pipeline congestion leads to the weak utilization and limited dispatch of GGs.

The natural gas supply curve of Case 2 for periods 1–24 is presented in Fig. 5 where supplier 1 with cheaper price provides more gas than supplier 2, logically. The day-ahead scheduling and allocating of natural gas for Case 2 is presented as Table VI and operating performance of SNGTs for periods 1–24 is profiled in Fig. 6. Generally, the working gas inventory fluctuation
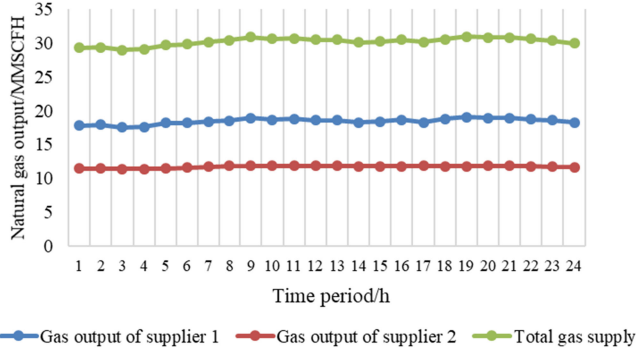
Fig. 5. Hourly natural gas supply of Case 2 in the IEEE 39-bus-15-node test IEGS.

TABLE VI
DAY-AHEAD NATURAL GAS SCHEDULING OF CASE 2 IN THE IEEE 39-BUS-15-NODE TEST IEGS

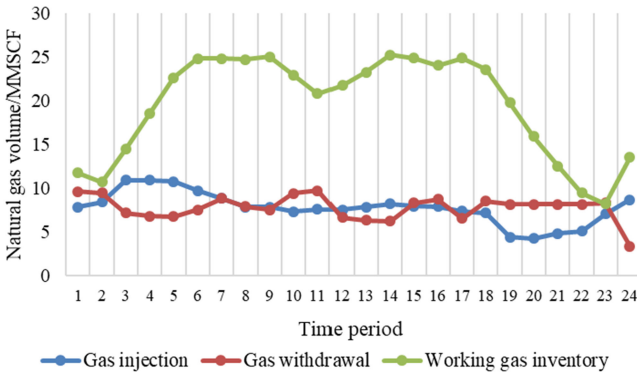| Period	Gas allocation (MMSCF)				
	Gas supply	Gas for load	Gas for power	Gas for storage	Gas for compressor
3	28.92	9.94	6.73	10.92	1.33
4	29.06	10.07	6.72	10.93	1.34
19	30.90	13.89	11.26	4.38	1.37
20	30.81	14.40	10.81	4.24	1.36
Whole day	724.54	298.14	207.86	186.08	32.46

Fig. 6. Hourly operating results for SNGTs of Case 2 in the IEEE 39-bus-15-node test IEGS.

of SNGTs is contrary to the gas load. SNGTs are net injected from IEGS with the decreasing gas load whereas net withdrawn to IEGS with the increasing gas load. Consequently, with the utilization of SNGTs, the gas demand of gas-fired reserve at the high load period is successfully transferred into the low load period, which effectively smoothes the gas supply curve shown in Fig. 5 and stores the surplus cheap gas for subsequent RR and SR demand.

The day-ahead optimal results of Cases 1–6 are compared in Table VII. RR demand is determined dominatingly by the forecast error of load and renewable power, so the sequential increment of predefined max forecast errors for Cases 1–3 leads to the inevitable increase of scheduled reserve and total energy cost. Compared Case 4 with Case 2, 12% increase of total cost

TABLE VII
DAILY RESULT COMPARISON OF DIFFERENT CASES IN THE IEEE 39-BUS-15-NODE TEST IEGS

Case	Power (10^4 MW)			Reserve (10^4 MW)			Gas (MMSCF)	Obj (10^6 $)
	Coal-fired	Gas-fired	Total	Coal-fired	Gas-fired	Total		
1	10.42	1.66	12.08	0.26	1.43	1.69	721.03	2.3589
2	10.40	1.68	12.08	0.43	1.41	1.84	724.54	2.3997
3	10.37	1.71	12.08	0.74	1.39	2.13	724.21	2.4789
4	10.42	1.66	12.08	0.43	1.41	1.84	715.17	2.6982
5	10.40	1.68	12.08	0.43	1.41	1.84	724.54	2.3997
6	8.81	3.27	12.08	0.00	1.84	1.84	961.53	1.9820

TABLE VIII
DATA OF GGS IN THE IEEE 118-BUS-40-NODE TEST IEGS

Type	Bus	Node	Max output (MW)	Ramp (MW /min)	Heat rate coefficient (MBtu/MWh)
1	56,92	35,37	100	6.0	9.0
2	24,27,99,103	3,6,38,40	150	9.0	8.5
3	54,55	13,34	150	9.0	9.0
4	25,26,49,100	4,7,12,39	300	18.0	7.0

and 1.3% decrease of scheduled natural gas are credible due to the higher gas price of Case 4. Without $N-1$ outages, Case 5 has been allocated the same reserve as Case 2, because SR capacity requirement is identical 600 MW for the whole day. However, to meet the $N-1$ criterion, the individual dispatch of CGs and GGs for Case 2 is different from Case 5. As aforementioned, the inadequate dispatch of GGs is caused by gas pipeline congestion in Case 2. Therefore, the transportation capacity of pipelines in Case 6 is expanded to 150%, leading to 33% increase of daily gas supply and 17% decrease of daily cost. Moreover, GGs at N14 are fully loaded in Case 6, greatly more than 37.5% loaded in Case 2.

B. IEEE 118-Bus-40-Node Test IEGS

1) Introduction of Test System and Cases: To further validate the effectiveness of the proposed method, MISOCP model with gas flow correction is also performed on a larger-scale test IEGS. Based on the primal IEEE 118-bus power system including 186 transmission lines, 3200 MW units are replaced by 12 GGs (details in Table VIII) with SNGTs, 1000 MW units are replaced by 10 renewable resources and the other 32 units (6688.2 MW) remained are CGs. The 40-node gas system, including 12 gas suppliers, 35 pipelines and 4 gas-powered compressors, is composed of two Belgium 20-node gas networks in [33] connected by the tie-pipeline N4-N40. The topology of the IEEE 118-bus-40-node test IEGS is depicted in Fig. 7. The price data of CGs and natural gas suppliers is presented in Table IX.

RR and SR capacity requirements and gas consumption coefficients of compressors are predetermined as same as IEEE 39-bus-15-node test IEGS. N1 is the pressure reference node at 900 Psia, the maximum $N-1$ generator outage (805.2 MW unit at B19) is considered, and the max forecast error is defined as the sum of 3% electricity load and 5% renewable power. Besides, the dispatch interval T is set as 2 h. Several cases are designed in Table X from more perspectives where C-electricity refers to the coal-fired electricity.
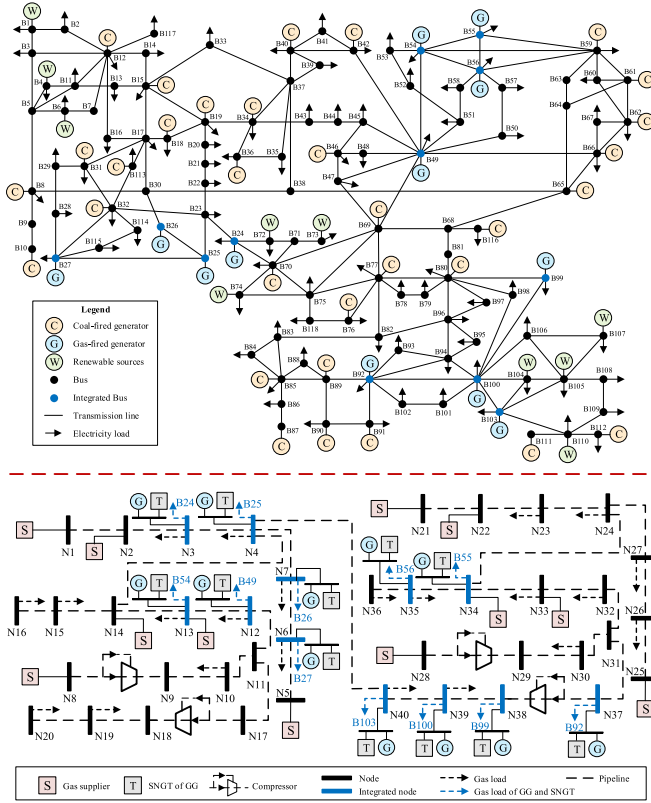
Fig. 7.   Topology of the IEEE 118-bus-40-node test IEGS.

TABLE IX
PRICE DATA OF CGs AND NATURAL GAS SUPPLIERS IN THE IEEE 118-BUS-40-NODE TEST IEGS

	Offering price of CGs ($/MWh)			Price of gas suppliers ($/MMSCF)	
Bus	Power	RR	SR	Node	Gas
8,12,15,18,19,31,32	30.0	42.0	35.0	1,21	1680
34,36,40,42,46,59,61	30.0	42.0	35.0	2,22	2280
62,70,76,77,85,87,90	30.0	42.0	35.0	5,25	2280
91,111-113,116	30.0	42.0	35.0	8,28	1680
10	28.5	34.0	30.5	13,33	2280
65,66	33.0	37.2	36.6	14,34	2280
69	35.0	29.0	26.0	-	-
80	27.8	36.4	32.1	-	-
89	26.0	32.8	29.5	-	-

TABLE X
CASES OF THE IEEE 118-BUS-40-NODE TEST IEGS

Case	CG price	Gas price	Higher price	Renewable capacity	Gas storage capacity
1	Base	Base	C-electricity	1000 MW	Base
2	Base	3.0 Base	Gas	1000 MW	Base
3	Base	Base	C-electricity	2000 MW	Base
4	Base	Base	C-electricity	2000 MW	1.5 Base

2) Effectiveness of the Proposed MISOCP Model With Gas Flow Correction Method: Based on Case 1 in Table X, the proposed MISOCP model is compared with the previous MISOCP and MILP models applied in Section IV.A. The comparison results are analyzed in Table XI. Similar to IEEE 39-bus-15-node test IEGS, the proposed MISOCP model also provides the

TABLE XI
COMPARISON ANALYSIS FOR MISOCP AND MILP MODELS WITH CASE 1 IN THE IEEE 118-BUS-40-NODE TEST IEGS

Method	Proposed MISOCP	Previous MISOCP	MILP-1	MILP-2
Obj (10^6 $)	4.8914	4.8914	4.8945	4.8917
Optimization time (Sec)	231.76	1171.66	261.61	385.97
Cones	420	420	-	-
Integers	420	420	3780	12180
Maxerr (%)	19.87	21.49	17.61	6.65

TABLE XII
FEASIBILITY OF GAS FLOW CORRECTION METHOD FOR THE PROPOSED MISOCP MODEL WITH DIFFERENT CASES IN THE IEEE 118-BUS-40-NODE TEST IEGS

Case	Obj (10^6 $)	Optimization time (Sec)	Correction time (Sec)	Maxerr (%)	Average iterations
1	4.8914	231.76	0.118	8.6×10^{-7}	5.08
2	11.1567	248.18	0.133	1.3×10^{-8}	5.58
3	4.6311	224.97	0.176	6.5×10^{-7}	5.50
4	4.6303	219.45	0.160	1.3×10^{-10}	5.83

TABLE XIII
DAILY RESULT COMPARISON OF DIFFERENT CASES IN THE IEEE 118-BUS-40-NODE TEST IEGS

Case	Power (10^4 MW)			Reserve (10^4 MW)			Gas (MMSCF)
	Coal-fired	Gas-fired	Total	Coal-fired	Gas-fired	Total	
1	3.973	3.665	7.638	0.386	1.855	2.241	2013.28
2	7.638	0.000	7.638	2.241	0.000	2.241	1586.82
3	3.037	3.603	6.640	0.374	1.917	2.291	2017.54
4	3.038	3.602	6.640	0.373	1.918	2.291	2017.21

minimum objective and presents the distinct advantage of higher computational efficiency than the previous MISOCP and MILP models for a larger-scale IEGS. Actually, due to the existing constraints of generator ramp and gas storage, the day-ahead dispatch model is a multi-period coupled optimization problem which is more dependent on a high-efficient algorithm.

Moreover, the gas flow correction procedure is employed for the proposed MISOCP model with different cases in Table X. Simulation results are shown in Table XII, which illustrate that the proposed correction method is effective for MISOCP model to ensure the exactness of dispatch results with few correction iterations and short calculation time. For these four various cases, the maximum $N-1$ generator outage and the max forecast error concerned are the same, so the optimization time of MISOCP models has a little difference.

3) Day-Ahead Dispatch Results of Test System: By the proposed MISOCP model with gas flow correction method, the optimal daily costs of different cases are solved and presented in Table XII and day-ahead dispatch results are compared in Table XIII.

For Case 1, the electricity load is almost averagely supplied by CGs and GGs whereas 83% reserve is provided by GGs, matching the assumption that natural gas price is lower,
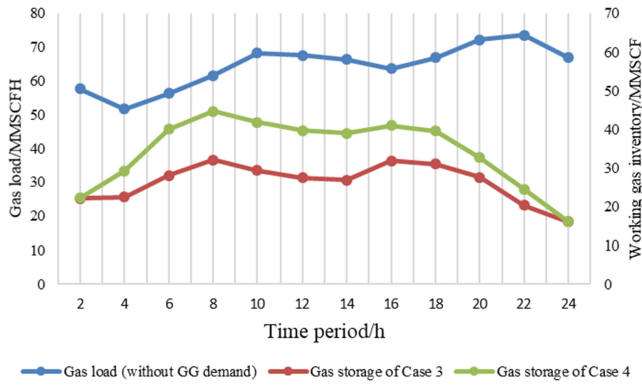
Fig. 8. Daily natural gas load (without GG demand) and working gas inventory of SNGTs for Case 3 and Case 4 in the IEEE 118-bus-40-node test IEGS.

especially for gas-fired reserve. Actually, all GGs in Case 1 are fully scheduled to satisfy the total demand of electricity load and reserve. However, the day-ahead dispatch result for Case 2 is opposite. The cheaper price and sufficient capacity of CGs lead to all coal-fired supply for electricity load and reserve without the use of GGs. Therefore, the energy utilization and unit dispatching are sensitive to the energy price. To discuss the impact of different renewable penetrance on IEGS dispatching, another 1000 MW CGs are replaced by renewable resources in Case 3. Compared with Case 1, the renewable power of Case 3 is twice, causing the less output of CGs and GGs for electricity load with a lower operational daily cost. Nevertheless, due to the increasing renewable power, IEGS requires a larger scheduled RR to withstand potential uncertainties.

For Case 3 and Case 4, the gas storage capacity is varied, and daily working gas inventories of SNGTs are profiled in Fig. 8. The initial gas inventory of SNGTs is 16 MMSCF and final gas inventories for two cases are both returned to 16 MMSCF, in accordance with the assumption that gas storage are balanced in a whole day. Compared with the day-ahead forecast natural gas load curve, SNGTs inject gas from IEGS during the low gas load periods and withdraw gas to IEGS during the high gas load periods, leading to a temporal transfer of reserve gas demand and a reduction of gas supply burden at peak hours. Moreover, with a larger storage capacity, the daily operation of SNGTs for Case 4 is different from Case 3. In Case 4, more cheap gas can be stored for reserve with the achievement of a more economic dispatching solution.

V. CONCLUSION

With renewable uncertainties and reserve scheduling, a robust day-ahead dispatch of IEGS was modeled in this paper. A novel SOC relaxation was presented considering uncertain gas flow directions to address the nonconvexity of Weymouth equation. Then the bi-level robust programming problem was mathematically reformulated into a standard MISOCP model with the introduced dummy variables. In order to guarantee the tightness of SOC relaxation, gas network solutions obtained from MISOCP model were corrected by the multi-slack-node gas flow calculation with Newton-Raphson method. Numerical

cases were performed on IEEE 39-bus-15-node test IEGS and IEEE 118-bus-40-node test IEGS, and several key findings are summarized following:

- Compared with MILP model, the proposed MISOCP model provided a more economic day-ahead dispatching solution with a shorter computational time;
- The proposed MISOCP model presented the superiority in narrower feasible region, higher computational efficiency, and wider application than the previous MISOCP model.
- The major barrier of MISOCP computational efficiency was the introduction of uncertainty and $N-1$ outage constraints;
- Due to the loop existence of test IEGSs, the maximum gas flow error of MISOCP results was over 13%, which were converged well in the gas flow execution, demonstrating the necessity and effectiveness of gas flow correction method;
- Based on the MISOCP model and gas flow correction, exact day-ahead dispatch solutions were available and sensitive to transmission congestion and price changes;
- The use of SNGTs led to the transfer of reserve gas demand from high to low load periods, beneficial for smoothing the gas supply curve, storing the surplus cheap gas for reserve and reducing the total operational cost.

Besides, due to the better objective optimum and the shorter computational time, the proposed MISOCP model can be also employed for other IEGS problems, such as optimal unified power and gas flow, long-term planning, real-time dispatching and market clearing.

REFERENCES

[1] K. Wang *et al.*, "A survey on energy internet: Architecture, approach, and emerging technologies," *IEEE Syst. J.*, to be published, doi: 10.1109/JSYST.2016.2639820.

[2] A. Quelhas, E. Gil, J. D. McCalley, and S. M. Ryan, "A multiperiod generalized network flow model of the U.S. integrated energy system: Part I—Model description," *IEEE Trans. Power Syst.*, vol. 22, no. 2, pp. 829–836, May 2007.

[3] National Energy Administration, "Background material for the action plan of internet plus smart energy," Jun. 24, 2016. [Online]. Available: http://fangtan.china.com.cn/2016-06/24/content_38738456_2.htm

[4] J. S. Andrepont, "Developments in thermal energy storage: Large applications, low temps, high efficiency, and capital savings," *Energy Eng.*, vol. 103, no. 4, pp. 7–18, 2006.

[5] Q. Li, S. An, and T. W. Gedra, "Solving natural gas loadflow problems using electric loadflow techniques," in *Proc. North Amer. Power Symp.*, 2003. [Online]. Available: http://pdfs.semanticscholar.org/42a4/a3b640398a6230ff0e42ac4c1b68f417dec3.pdf

[6] A. Martinez-Mares and C. R. Fuerte-Esquivel, "A unified gas and power flow analysis in natural gas and electricity coupled networks," *IEEE Trans. Power Syst.*, vol. 27, no. 4, pp. 2156–2166, Nov. 2012.

[7] S. Chen *et al.*, "Multi-linear probabilistic energy flow analysis of integrated electrical and natural-gas systems," *IEEE Trans. Power Syst.*, vol. 32, no. 3, pp. 1970–1979, May 2017.

[8] Y. Hu *et al.*, "Unified probabilistic gas and power flow," *J. Mod. Power Syst. Clean Energy*, vol. 5, no. 3, pp. 400–411, 2017.

[9] C. Unsihuay-Vila *et al.*, "A model to long-term, multiarea, multistage, and integrated expansion planning of electricity and natural gas systems," *IEEE Trans. Power Syst.*, vol. 25, no. 2, pp. 1154–1168, May 2010.

[10] C. A. Saldarriaga, R. A. Hincapié, and H. Salazar, "A holistic approach for planning natural gas and electricity distribution networks," *IEEE Trans. Power Syst.*, vol. 28, no. 4, pp. 4052–4063, Nov. 2013.

[11] Y. Hu, Z. Bie, T. Ding, and Y. Lin, "An NSGA-II based multi-objective optimization for combined gas and electricity network expansion planning," *Appl. Energy*, vol. 167, pp. 280–293, 2016.

[12] C. Liu, M. Shahidehpour, Y. Fu, and Z. Li, "Security-constrained unit commitment with natural gas transmission constraints," *IEEE Trans. Power Syst.*, vol. 24, no. 3, pp. 1523–1536, Aug. 2009.

[13] H. Khani and H. E. Z. Farag, "Optimal day–ahead scheduling of power–to–gas energy storage and gas load management in wholesale electricity and gas markets," *IEEE Trans. Sustain. Energy*, vol. 9, no. 2, pp. 940–951, Apr. 2018.

[14] A. Alabdulwahab, A. Abusorrah, X. Zhang, and M. Shahidehpour, "Coordination of interdependent natural gas and electricity infrastructures for firming the variability of wind energy in stochastic day-ahead scheduling," *IEEE Trans. Sustain. Energy*, vol. 6, no. 2, pp. 606–615, May 2015.

[15] A. Alabdulwahab, A. Abusorrah, X. Zhang, and M. Shahidehpour, "Stochastic security-constrained scheduling of coordinated electricity and natural gas infrastructures," *IEEE Syst. J.*, vol. 11, no. 3, pp. 1674–1683, Sep. 2017.

[16] X. Zhang, M. Shahidehpour, A. Alabdulwahab, and A. Abusorrah, "Hourly electricity demand response in the stochastic day-ahead scheduling of coordinated electricity and natural gas networks," *IEEE Trans. Power Syst.*, vol. 31, no. 1, pp. 592–601, Jan. 2016.

[17] F. Wang and K. W. Hedman, "Dynamic reserve zones for day-ahead unit commitment with renewable resources," *IEEE Trans. Power Syst.*, vol. 30, no. 2, pp. 612–620, Mar. 2015.

[18] A. Street, A. Moreira, and J. M. Arroyo, "Energy and reserve scheduling under a joint generation and transmission security criterion: An adjustable robust optimization approach," *IEEE Trans. Power Syst.*, vol. 29, no. 1, pp. 3–14, Jan. 2014.

[19] W. Wei, F. Liu, S. Mei, and Y. Hou, "Robust energy and reserve dispatch under variable renewable generation," *IEEE Trans. Smart Grid*, vol. 6, no. 1, pp. 369–380, Jan. 2015.

[20] Y. Tang, C. Luo, J. Yang, and H. He, "A chance constrained optimal reserve scheduling approach for economic dispatch considering wind penetration," *IEEE/CAA J. Automat. Sin.*, vol. 4, no. 2, pp. 186–194, Apr. 2017.

[21] X. Ma, Y. Chen, and J. Wan, "Midwest ISO co-optimization based real-time dispatch and pricing of energy and ancillary services," in *Proc. IEEE Power Energy Soc. Gen. Meeting*, Calgary, AB, Canada, 2009, pp. 1–6.

[22] C. Shao, X. Wang, M. Shahidehpour, X. Wang, and B. Wang, "An MILP-based optimal power flow in multicarrier energy systems," *IEEE Trans. Sustain. Energy*, vol. 8, no. 1, pp. 239–248, Jan. 2017.

[23] C. M. Correa-Posada and P. Sanchez-Martin, "Gas network optimization: A comparison of piecewise linear models," 2017. [Online]. Available: http://pdfs.semanticscholar.org/9226/1ed0f303642270fe6b23a71eef30 adbcbb43.pdf.

[24] Y. He, M. Shahidehpour, Z. Li, C. Guo, and B. Zhu, "Robust constrained operation of integrated electricity-natural gas system considering distributed natural gas storage," *IEEE Trans. Sustain. Energy*, to be published, doi: 10.1109/TSTE.2017.2764004.

[25] C. Wang, W. Wei, J. Wang, L. Bai, Y. Liang, and T. Bi, "Convex optimization based distributed optimal gas-power flow calculation," *IEEE Trans. Sustain. Energy*, to be published, doi: 10.1109/TSTE.2017.2771954.

[26] C. Borraz-Sanchez, R. Bent, S. Backhaus, H. Hijazi, and P. Hentenryck, "Convex relaxations for gas expansion planning," *Informs J. Comput.*, vol. 28, no. 4, pp. 645–656, 2016.

[27] Y. Wen, X. Qu, W. Li, X. Liu, and X. Ye, "Synergistic operation of electricity and natural gas networks via ADMM," *IEEE Trans. Smart Grid*, to be published, doi: 10.1109/TSG.2017.2663380.

[28] Y. He *et al.*, "Decentralized optimization of multi-area electricity-natural gas flows based on cone reformulation," *IEEE Trans. Power Syst.*, to be published, doi: 10.1109/TPWRS.2017.2788052.

[29] T. Ding, Z. Wu, J. Lv, Z. Bie, and X. Zhang, "Robust co-optimization to energy and ancillary service joint dispatch considering wind power uncertainties in real-time electricity market," *IEEE Trans. Sustain. Energy*, vol. 7, no. 4, pp. 1547–1557, Oct. 2016.

[30] R. A. Jabr, "Adjustable robust OPF with renewable energy sources," *IEEE Trans. Power Syst.*, vol. 28, no. 4, pp. 4742–4751, Nov. 2013.

[31] C. M. Correa-Posada and P. Sánchez-Martín, "Integrated power and natural gas model for energy adequacy in short-term operation," *IEEE Trans. Power Syst.*, vol. 30, no. 6, pp. 3347–3355, Nov. 2015.

[32] C. Borraz-Sánchez and R. Z. Ríos-Mercado, "Improving the operation of pipeline systems on cyclic structures by tabu search," *Comput. Chem. Eng.*, vol. 33, pp. 58–64, 2009.

[33] D. D. Wolf and Y. Smeers, "The gas transmission problem solved by an extension of the simplex algorithm," *Manage. Sci.*, vol. 46, no. 11, pp. 1454–1465, 2000.

Fan Liu (S'17) received the B.S. degree in 2015 from Xi'an Jiaotong University, Xi'an, China, where she is currently working toward the Ph.D. degree. Her major research interests include power system optimization and Energy Internet market.

Zhaohong Bie (M'98–SM'12) received the B.S. and M.S. degrees from Shandong University, Jinan, China, in 1992 and 1994, respectively, and the Ph.D. degree from Xi'an Jiaotong University, Xi'an, China, in 1998. Currently, she is a Professor with Xi'an Jiaotong University. Her main research interests include power system planning and reliability evaluation, integration of the renewable energy, as well as Energy Internet.

Xu Wang (S'16) received the B.S. degree from Tsinghua University, Beijing, China, in 2016. He is currently working toward the Ph.D. degree at Xi'an Jiaotong University, Xi'an, China. His major research interests include the co-optimization planning of integrated electricity and natural gas network.